OmpT: Molecular Dynamics Simulations of an Outer Membrane Enzyme

Marc Baaden, Mark S.P. Sansom

OmpT: Molecular Dynamics Simulations of an Outer Membrane Enzyme

Marc Baaden[1,2] and Mark S.P. Sansom[1,#]*

[1]Laboratory of Molecular Biophysics,
Department of Biochemistry,
University of Oxford,
South Parks Road,
Oxford,
OX1 3QU,
U.K.

Current addresses:

[2]Laboratoire de Biochimie Théorique,
CNRS UPR 9080,
Institut de Biologie Physico-Chimique,
13, rue Pierre et Marie Curie,
F-75005 Paris,
France.

[#]To whom correspondence should be addressed at:

e-mail: mark.sansom@biop.ox.ac.uk
Tel: +44-1865-275371
Fax: +44-1865-275182

Abstract

Five MD simulations (total duration >25 ns) have been performed on the *E. coli* outer membrane protease OmpT embedded in a DMPC lipid bilayer. Globally the protein is conformationally stable. Some degree of tilt of the β-barrel is observed relative to the bilayer plane. The greatest degree of conformational flexibility is seen in the extracellular loops. A complex network of fluctuating H-bonds is formed between the active site residues, such that the Asp210-His212 interaction is maintained throughout, whilst His212 and Asp83 are often bridged by a water molecule. This supports a catalytic mechanism whereby Asp83 and His212 bind a water molecule which attacks the peptide carbonyl. A configuration yielded by docking calculations of OmpT simulation snapshots and a model substrate peptide Ala-Arg-Arg-Ala was used as the starting point for an extended Hückel calculation on the docked peptide. These placed the LUMO mainly on the carbon atom of the central C=O in the scissile peptide bond, thus favouring attack on the central peptide by the water held by residues Asp83 and His212. The trajectories of water molecules reveal exchange of waters between the intracellular face of the membrane and the interior of the barrel but no exchange at the extracellular mouth. This suggests that the 'pore-like' region in the centre of OmpT may enable access of water to the active site 'from below'. The simulations appear to reveal the presence of specific lipid interaction sites on the surface of the OmpT barrel. This reveals the ability of extended MD simulations to provide meaningful information on protein/lipid interactions.

Introduction

Bacterial outer membrane proteins (OMPs) all share a common architecture, that of a transmembrane domain formed by an anti-parallel β-barrel. Up to date the structures of 20 such OMPs have been solved by X-ray diffraction (Buchanan, 1999; Koebnik et al., 2000) and by NMR (Arora et al., 2001; Fernandez et al., 2001). Thus, OMPs provide an opportunity for molecular dynamics (MD) simulation studies to explore the conformational dynamics of a whole family of structurally related membrane proteins, in order to define both common dynamic properties and functionally important differences between individual species of OMPs (Domene et al., 2003a; Bond and Sansom, 2004).

Perhaps the best characterised family of OMPs are the porins (Cowan, 1993; Schirmer, 1998; Achouak et al., 2001). These include both relatively non-specific general diffusion pores and also more specific passive pores (e.g. for oligosaccharides (Schirmer et al., 1995; Forst et al., 1998)) across the outer membrane. Thus, they are an important component of the transport properties of the bacterial membrane. Other transport proteins in outer membranes include those for ferric ions (Locher et al., 1998; Ferguson et al., 1998; Buchanan et al., 1999) and for vitamin B_{12} (Chimento et al., 2003), and export pathways for polypeptide toxins and hydrophobic drugs such as TolC (Koronakis et al., 2000).

In addition to transport proteins, outer membranes include a number of membrane bound enzymes. Several structures of such enzymes have been determined, including those of a protease OmpT (Vandeputte-Rutten et al., 2001), and two OMPs acting on lipid substrates, OMPLA (Snijder et al., 1999) and PagP (Hwang et al., 2002).

In the present work we focus on OmpT, the *Escherichia coli* outer membrane endoprotease Omptin (EC 3.4.21.87), which shows maximum enzymatic activity for cleavage sites with two consecutive basic amino acids (Arg-Arg, Lys-Arg, Lys-Lys) (Sugimura and Nishihara, 1988). OmpT also cleaves a number of more remote sequences as has been shown by

activity assays and library screening (Dekker et al., 2001). It is functional as a monomer and has an autoproteolytic site at K217-R218. Mutation of the three residues S99, G216 and K217 was a prerequisite for the crystallographic structure determination (Vandeputte-Rutten et al., 2001). The OmpT crystal structure comprises 297 amino acids and has revealed its prolonged 10-stranded beta-barrel architecture with a central elliptical crosssection of ca. 13 x 16 Å. The active site sits in the extracellular half of the structure at the base of two long loops that protrude from the barrel flanking a central binding pocket. Four residues have been identified as essential part of the active site, D210/H212 on one side of the pocket and D83/D85 on the opposite side. The biological function of OmpT is not fully established, but it may have a protective role in pathogenic *E. coli*. OmpT degrades a variety of positively charged antimicrobial peptides and might be involved in urinary tract disease and DNA excision repair.

MD simulations provide a valuable tool for studying membrane proteins, enabling us to probe their conformational dynamics in both membrane and detergent micelle environments (Bond and Sansom, 2003). They are of particular value in enabling us to extrapolate from the essentially static (time and space averaged) structure revealed by X-ray diffraction to a more dynamic picture of the behaviour of a single OMP molecule in a more realistic environment mimicking a small patch of the bacterial membrane. MD simulations have been employed in a number of studies of OMPs, most notably to probe protein and solvent dynamics in relationship to permeation mechanisms in porins (Tieleman and Berendsen, 1998; Im and Roux, 2002), to explore possible pore gating mechanisms in OmpA (Bond et al., 2002; Bond and Sansom, 2003), to explore dynamics in relationship to transport in FhuA (Faraldo-Gómez et al., 2003), and to examine the role of calcium binding and dimerisation in the catalytic mechanism of OMPLA (Baaden et al., 2003).

In the current study we employ MD simulations to examine the conformational dynamics of the active site of the outer membrane protease OmpT. We also explore the interactions of

OmpT with phospholipid molecules, which is of some interest in the context of possible specific interactions of OmpT with lipid A and their role in stability and/or function of OmpT.

Methods

System Preparation

Repair of protein structures

We started from chain A of the 2.6 Å crystal structure (PDB code 1i78) where missing sidechain atoms were modelled using a rotamer library (Chinea et al., 1995). We reversed the mutations required for the crystallization of OmpT: A99S, K216G and G217K.

pK_A Calculations

It has been our experience [66] that more stable MD simulations can be obtained if pK_A calculations are used to aid assignment of ionisation states to acidic and basic residues in a protein. Thus, pK_A calculations for OmpT were performed using the program WhatIf [67]. This approach combines calculation of the energies of different protonation states of ionisable residues via the Poisson-Boltzmann equation with modelling of local structural changes associated with (de)protonation of ionisable residues (Nielsen and Vriend, 2001). To mimic the dielectric environment presented by a membrane pK_A calculations were performed on OmpT embedded in a slab of methane molecules. The result was a series of titration curves for each ionisable residue, from which protonation states were assigned.

Insertion into a Bilayer

OmpT was inserted into a pre-equilibrated, hydrated (65 waters per lipid molecule) DMPC bilayer using the methods described by Faraldo-Gómez et al. (Faraldo-Gómez et al., 2002). Briefly, a hole of approximately the same size as the protein is made in the lipid bilayer by removal of DMPC molecules. A simulation is then run in which the lipid molecules at the edge of the hole experience local forces perpendicular to a molecular surface generated from the

protein to be inserted. This allows the lipids to relax around a protein-shaped cavity into which the protein is then introduced. Na^+ and Cl^- ions equivalent to a concentration of ca. 0.1 M were then added. A typical view of the total simulation system is shown in Fig. 1C.

Simulations

All simulations were performed using GROMACS 3.1.4. (Berendsen et al., 1995) The force field used was GROMOS-87. (van Gunsteren and Berendsen, 1987) The SPC water model was employed. (Berendsen et al., 1981) The simulations were run in the NPT ensemble. The temperature was maintained at 310 K using a Berendsen thermostat (Berendsen et al., 1984) with τ = 0.1 ps. The pressure was maintained at 1 bar by anisotropically coupling x, y and z components to a Berendsen barostat (Berendsen et al., 1984) with τ = 1.0 ps and compressibility of 4.5 10^{-5} bar^{-1} in all three dimensions. The time step for integration was 2 fs, and coordinates were saved every 1 ps for subsequent analysis. Electrostatic interactions were calculated using either: a cutoff of 18 Å and van der Waals interactions were truncated at 14 Å; or with PME (Darden et al., 1993) using a 10 Å cutoff for both the real-space calculation and the van der Waals interactions. The LINCS algorithm (Hess et al., 1997) was used to constrain all bond lengths.

Following insertion of the protein into the bilayer (see above) an equilibration simulation was performed during which restraints on the protein atoms were gradually released. This equilibration period was 0.6 ns. Production simulations of up to 10 ns duration were then performed.

Peptide Docking

Docking calculations of the three peptides ARRA, AKKA and AK(D)RA were performed with autodock3 (Morris et al., 1998) for seven protein conformations, identified by cluster analysis of all trajectories. In a second round we focused on one of the protein conformations, where protonation states were changed to better reflect a potential transition state,

Asp83 being protonated and His212 neutral. A water molecule was explicitly added between Asp83 and His212. We selected one of the ARRA complexes and refined sidechain positions interactively with the Yasara software (Krieger et al., 2002). Protein-substrate interactions were analysed with the program LIGPLOT (Wallace et al., 1995). The STC software (Lavigne et al., 2000) was used to estimate the free energies of active site/peptide interactions via a structure-based thermodynamic approach. Given the simple docking procedure used, the approximate nature of the resulting complex and the short length of the peptide, we only derived relative contributions of protein sidechains to the binding energy.

Additional Analysis Programs

Secondary structure elements were identified using the program DSSP (Kabsch and Sander, 1983), graphical representations were prepared with VMD (Humphrey et al., 1996) and Raster3D (Merritt and Bacon, 1997). Water bridges were identified with an adapted Gromacs analysis program provided by JD Faraldo-Gómez. Lipid-protein interactions were analysed using the Proximus database and associated tools (Deol and Sansom, unpublished results).

Results

Simulations and Stability

The simulation system, consisting of an OmpT monomer embedded in a DMPC bilayer, is shown in Fig. 1. In determining the initial configuration of this system, attention was paid to the location of the bands of amphipathic aromatic amino acid (i.e. Trp and Tyr) sidechains on the surface of the β-barrel, as it is thought that such residues help to 'lock' integral membrane proteins within a lipid bilayer (Killian and von Heijne, 2000; Lee, 2003; Fyfe et al., 2001). The other class of residues that have been suggested to interact with lipid headgroups are basic sidechains. In this context it is noteworthy that there are many basic residues in the upper (i.e.

extracellular) half of the OmpT barrel, pointing out towards the lipid headgroups (Fig. 1A: also see discussion below).

Five simulations were performed (Table 1). OMPT1 and OMPT2 were both of 10 ns duration, but differed in the manner in which long-range electrostatic interactions were approximated. OMPT3a-c were short (2.5 ns) reruns of the OMPT2 simulation using different random seeds and starting conformations. By performing multiple simulations we aimed to explore the robustness of our results to changes in simulation protocol (OMPT1 vs. OMPT2) and to stochastic fluctuations and differences between multiple runs of a given simulation protocol. Furthermore, better sampling is achieved by multiple simulation runs (Caves et al., 1998).

Visualisation of the results of e.g. simulation OMPT2 (Fig. 1C) suggests that whilst there is no overall translation of the OmpT β-barrel relative to the lipid bilayer, some degree of tilting occurs. This is discussed in more detail below. However, extended simulations of phospholipid bilayers have revealed surface undulations (Lindahl and Edholm, 2000) and so we cannot exclude the possibility of similar long (i.e. >> 10 ns) timescale fluctuations in OMP orientations in membranes.

The overall drift of OmpT from the initial (i.e. crystallographic) structure provides a measure of the conformational stability of this protein in a membrane environment. Drift can be simply measured in terms of the Cα root mean square deviation (RMSD) from the starting structure. In both simulations OMPT1 and OMPT2 (Fig. 2) it can be seen that the β-barrel is very stable, with a final Cα RMSD of ~1 Å, whereas the highest degree of structural drift is seen in the loop regions, for which the cutoff simulation (i.e. OMPT2) may show a slightly higher degree of drift on a 10 ns timescale.

Detailed analysis of the convergence of the simulations using principle components analysis (PCA) and other methods will be published elsewhere (Faraldo-Gómez et al., 2004). To summarize, the OmpT simulations were among the best converged systems comparing 9

different membrane proteins in a lipid environment. The similarity of both halves of the simulation – a measure for the sampling completeness – derived from PCA is 81 % for the transmembrane part and 66 % for the whole protein. This compares very favourably to shorter simulations of the OmpF porin with values from 12 to 16 % (Hess, 2002). The structural drift of the backbone of the four active site residues was found to be less than 1 Å.

Analysis of the radius of gyration confirms that OmpT is a stable protein in multinanosecond simulations and suggests some degree of tilting of OmpT in the bilayer, which is more pronounced with OMPT1. More exact protein tilt analysis confirms the significant tilting of OmpT in the bilayer (this is discussed below). Overall, the simulations confirm that, despite the low resolution (2.6 Å), the OmpT structure is remarkably stable in simulations on a ~10 ns timescale.

Conformational Fluctuations

Whilst the OmpT structure is globally stable in the simulations, this is not to imply that no significant conformational fluctuations take place. Thus, it is of interest to also examine the magnitude of the conformational fluctuations in different regions of the structure and to compare these with the experimental B-values (whilst not forgetting the resolution of the structure, namely 2.6 Å). In Fig. 3A the Cα root mean square fluctuations (RMSFs) are shown as a function of residue number for OMPT1, and compared with the equivalent RMSFs derived from the B-values. Qualitatively the two curves agree, with the highest fluctuations being seen in the extracellular loops and the lowest fluctuations in the core of the β-strands. Two major differences are observed. Firstly the peak values of the RMSFs for the loops are higher in the simulation than in the crystal structure. This may reflect constraints on loop mobility present in the crystal which are removed when the protein is in a bilayer. Such an interpretation is supported by recent simulations of the small outer membrane protein OmpA in a crystal vs. a bilayer environment (Bond and Sansom, ms. in preparation). The second major difference is that the RMSFs derived

from the B-values are significantly higher than those seen in the simulations for the core regions of the β-barrel. This probably reflects some contribution of static crystal disorder (e.g. mosaicity) to the B-values as well as undersampling of long-timescale motions of the barrel (Faraldo-Gómez et al., 2004).

We have also examined the Cα RMSF values as a function of the *z* coordinate of the Cα atoms (i.e. the position of the Cα atom projected onto the approximate bilayer normal). For all three simulations this analysis (data not shown) reveals a similar pattern to that seen in other outer membrane protein simulations (Bond and Sansom, 2004), namely the RMSFs are lowest (~0.6 Å) in the centre of the membrane (also the middle of the barrel) and rise at either end, being highest in the extramembraneous loops.

Visualisation (Fig. 3B) of superimposed snapshots taken throughout the simulations suggests that the pattern of mobility defines two relatively rigid 'halves' of the barrel, with highly mobile extracellular loops (two of which contain the active site residues sitting at the region connecting with the barrel) flanking a potential peptide binding site in between. This poses the question of the possible role(s) of such loop flexibility in the catalytic mechanism of OmpT. One possibility is that the mobile loops enhance (i.e. lower the activation energy for) entry/exit of substrate/product from the active site.

We have also monitored the secondary structure as a function of time for each simulation. Comparing the three simulations (i.e. treating the OMPT3a-c simulations together) and examining the predominant secondary structure for each residue during each simulation (Fig. 3C), one can see that differences in secondary structure between the three simulations are only observed for the extracellular loops, in agreement with the pattern of fluctuations described above.

The Active Site

The mechanism proposed for OmpT has active site residues located on two extracellular loops on opposite faces of the barrel (cf. Fig. 1A), namely a His212-Asp210 dyad on one side of the proposed peptide binding site, and an Asp83-Asp85 couple on the other side. The His212-Asp210 dyad is thought to activate a water molecule for nucleophilic attack on the C of the peptide bond whilst the Asp83-Asp85 couple may have a dual role, both by coordinating and thus helping to orient the nucleophilic water (Vandeputte-Rutten et al., 2001) and possibly by stabilizing the oxyanion intermediate via a shared proton (Kramer et al., 2001). Earlier mutagenesis studies (Kramer et al., 2000) had suggested a role for Ser99 although this is less clear in terms of the structure. It has been suggested (Kramer et al., 2001) that Glu27 and Asp208 may also play a role in substrate binding via interaction with a substrate arginine sidechain. The simulations of OmpT provide an opportunity to examine the structural integrity of the active site and the nature of the interactions between the key residues as they evolve over time, and in particular to explore the interactions of water molecules with active site sidechains.

There is a complex network of H-bonds (Fig. 4A/B) between the active site residues, which fluctuates as a function of time (Fig. 4C; Table 2). Firstly, in all of the simulations the Asp210-His212 H-bonding interaction is maintained throughout. His212 and Asp83 are often bridged by a water molecule (Fig. 4) thus supporting the mechanism of (Kramer et al., 2001) where Asp83 and His212 are proposed to bind the water which goes on to attack the peptide carbonyl. Occasionally, Asp83 and His212 are bridged by a chain of two water molecules. Interestingly, the Asp83-water-His212 interaction is sometimes replaced by an Asp83-Ser99 interaction. The loss of enzyme activity on mutating Ser99 to Ala suggests that this alternative Asp-Ser interaction may play a functionally important role. The Asp83-Asp85 pair interact with one another via one or more bridging water molecules. Finally, Glu27 switches between interacting with Asp208 directly and with Asp210 via an intervening water. Thus, water molecules seem to play an important role in the active site, both in terms of being a possible

component of the catalytic mechanism *per se* (the water(s) held by His212 and Asp83) and by bridging between sidechains to maintain the integrity of the active site. Of course, these simulations are in the absence of bound peptide substrate, and a different configuration of sidechains and waters may be expected in the latter state.

As part of the preparation of the simulation system (see Methods) we performed pK_A calculations. These suggested that His212 protonation was favoured by ~10% at neutral pH (the calculated pK_A was ~7.9). In combination with the results of the H-bonding analysis discussed above, this might suggest that a proton transfer shuttle between water, His212 and Asp83 may play a key role in the catalytic mechanism. Interestingly, the pK_A calculations also suggested that the pK_A of Asp85 was perturbed from its standard value (to ~6.6).

The simulations were all performed in the absence of bound peptide substrate. In order to explore the influence of active site fluctuations on enzyme-substrate interactions we have performed docking simulations (see Methods section) between selected OmpT snapshots from the simulations and three model peptides: Ala-Lys-Lys-Ala, Ala-Arg-Arg-Ala, and Ala-Lys-(D)Arg-Ala. The first two are models of substrates, whereas the third peptide is an inhibitor. The results from docking these peptides to different snapshots of OmpT from the simulations provide a range of complexes. Some of the observed configurations are compatible with the catalytic mechanisms discussed and place the peptide cleavage site near the catalytic residues. However, the precision of the docking calculation does not permit a detailed insight into the mechanism as several alternative docked structures are close to one another in energy. In Fig. 5 we show an interactively refined docked complex of Ala-Arg-Arg-Ala with the active site configuration from simulation OMPT1 at 0 ps. It can be seen that the scissile peptide bond is located between the Asp83-Asp85 and Asp210-His212 pairs. This conformation was chosen, because a water molecule was present between His212 and Asp83. The water is supposed to perform the nucleophilic attack. In order to take into account the effect of a second water between Asp83 and

Asp85, we protonated Asp83, which is therefore able to provide a proton for the stabilization of the oxyanion produced during hydrolysis. The N-terminal Arg of the peptide interacts with Glu27 (distance 2.8 Å) and Asp208 (distance 3.0 Å) and the C-terminal Arg with Asp97 (distance 3.1 Å). Furthermore the N-terminal Ala interacts with Met81 and Ile170 as has been hypothesized previously (Vandeputte-Rutten et al., 2001). Thus the results of the docking are consistent with the mechanism proposed on the basis of the crystal structure and mutagenesis studies.

Another interesting feature of the OmpT active site are the fluctuations of the putative peptide binding cleft, in particular the hot spot delineated by the four residues D83, D85, N210 and H212. One flexibility measure is the evolution of the H212-D83 and H212-D85 distances vs. time, which fluctuate between 3 and 8 Å (graphs not shown) and show a clear bimodal distribution with maxima at 4.0 and 5.6 Å in simulation OMPT2.

To further examine the peptide docked at the active site we performed an extended Hückel calculation on the Ala-Arg-Arg-Ala peptide in the docked conformation discussed above. The results of this calculation (data not shown) placed the LUMO mainly on the carbon atom of the central C=O in the scissile peptide bond. A control calculation on an energy minimized conformation of the isolated peptide – with no docking constraints – placed the LUMO in a different position incompatible with the expected enzymatic reaction. Thus the docked conformation seems to favour attack on the central peptide bond and the preferred direction of attack would seem to be from "below", i.e. from the direction of the water held by residues Asp83 and His212.

The results of a thermodynamic analysis (described in the Methods section) of the peptide/OmpT complex shown in Fig. 5 suggests that the predominant interactions between the peptide and the binding site include those of Glu27 and Asp210, but also, more surprisingly, those of Tyr150, Arg168, Lys217 and Tyr221.

The results of our simulations seem to be broadly compatible with suggested mechanism(s) (Kramer et al., 2001). In particular, we have evidence for the stability of the Asp210-His212 dyad, and for the presence of one - occasionally two - bridging water molecules held by His212 and Asp83. This strongly suggests that the water molecule held by His212 and activated by the catalytic dyad is 'poised' to attack the scissile peptide bond, the peptide being oriented such that its LUMO is directed towards the water oxygen. As to the stabilizing role of Asp83 and Asp85, several possibilities can be considered. Firstly, the water held between Asp83 and Asp85 may act as the donor of a shared proton between these two residues, in agreement with the mechanism proposed by (Kramer et al., 2001). Secondly, the attacking water molecule could simultaneously provide a proton to stabilize the oxyanion intermediate and hydrolyse the peptide bond. Thirdly, if two water molecules were bridging, one could play a stabilizing role whilst the other acts as a nucleophile.

Water

The crystal structure of OmpT reveals between 6 and 9 waters within the OmpT barrel (depending on which of the two monomers in the asymmetric unit one examines). Given the behaviour of water molecules within the pore-like β-barrel of OmpA we were interested to examine the dynamic properties of water within the OmpT barrel. In particular, we wished to examine whether the water inside the β-barrel behaved simply as a 'structural' element or whether OmpT could form a potential water permeable pore through the outer membrane.

The time average distribution of water molecules inside the barrel (Fig. 6A) indicates that water can access most of the interior of the barrel but that there is a region of low water density around the extracellular mouth of the barrel. This low water density region corresponds to the narrowest region of the barrel in the crystal structure, where the barrel is 'squashed' such as to have a highly elliptical cross-section. If we examine the trajectory of a single (typical) water molecule (Fig. 6B) we can see ready exchange of the water molecule between the intracellular

face of the membrane and the interior of the barrel but no exchange of water at the extracellular mouth. This is supported by following the trajectories of a number of water molecules within the barrel projected onto the *z* (i.e. approximate barrel) axis (Fig. 6C).

What does this mean in terms of the function of OmpT? One is tempted to speculate that the 'pore-like' region in the centre of the OmpT molecule may allow access of water to/from the active site 'from below' i.e. on the side of the active site facing towards the interior of the β-barrel just beneath the putative peptide binding site.

Lipid/Protein Interactions

The OMPT simulations provide an opportunity to explore further the nature of lipid-protein interactions in a lipid bilayer mimicking the bacterial outer membrane and the extent to which these may be characterised by simulations. This is a topic of some general importance, as an improved understanding of protein/lipid interactions may enable us to better predict the structure of membrane proteins. Furthermore, interactions between lipid molecules and membrane proteins are known to play important roles in the stability and structural integrity of membrane proteins (Killian and von Heijne, 2000; Lee, 2003). Furthermore, OmpT requires LPS for its function and on the basis of structural comparisons with FhuA (Ferguson et al., 1998) it has been suggested that there may be a specific LPS binding site on the surface at the extracellular end of the OmpT β-barrel (Vandeputte-Rutten et al., 2001).

As discussed briefly above we have observed a degree of tilting of the OmpT barrel relative to the lipid bilayer. For example, at the end of simulation OMPT1 the barrel axis is tilted ~20º relative to the (overall) bilayer plane. We have seen a similar tilting of the barrel of the simple outer membrane protein OmpA (Bond et al., 2002) and a similar tilting of OmpA has been predicted by (Basyn et al., 2001) using a simplified potential for protein/membrane interactions. We therefore suggest that the tilt of OmpT may reflect an underlying asymmetry in the interaction of the outer barrel envelope with the bilayer. This is suggested by the agreement

between the tilt seen in MD simulations and that generated using a simple hydrophobicity potential for sidechain/bilayer interactions (Deol & Sansom, unpublished results). It is possible that the development of the tilt of OmpT relative to the bilayer during the simulations may be related to the increase in the number of lipid/protein H-bonds observed during the early stages of both simulations OMPT1 and OMPT2 (Fig. 7).

This increase in number of H-bonds is suggested to correspond to a slow (> 2 ns) optimisation of the interaction of the protein with the bilayer. Similar timescales for fluctuations of number of protein/lipid interactions have been observed in simulations of OmpA and KcsA (Domene et al., 2003b).

As mentioned above, on the basis of comparing the crystal structures of FhuA (with bound LPS; PDB code 1QFG) and of OmpT, (Vandeputte-Rutten et al., 2001) suggested a LPS binding site for OmpT. This consisted of OmpT residues Tyr134, Glu136, Arg138, Arg175 and Lys226. In the FhuA structure the primary contacts from the protein to the Lipid A portion of LPS are via a lysine and arginine cluster to the diphosphate moiety and via a lysine and glutamine cluster to the single phosphate (Fig. 8A).

We have analysed the principal contacts between the phosphate of DMPC and the OmpT sidechains of the proposed LPS binding site, of the nearby Lys177 and of a second possible LPS site identified by examination of snapshots from the simulations. The results of this analysis are summarised in Table 3 and some snapshots are shown in Fig. 8B. From the table we can see that there are long-lasting (i.e. >8% of the duration of a given simulation) H-bonds from the DMPC molecules to all of the residues in the proposed LPS binding site in at least one simulation. The analysis suggests that the proposed site may also have an affinity for the phosphate part of the PC headgroup. The simulations also suggest that Lys177 may play a role in this binding site. Interestingly, residues Tyr134, Glu136, Arg138, Arg175 *and* Lys177 form interactions with the detergent molecules (β-octylglucoside) present in the OmpT crystal structure. This would

suggest that this region of the OmpT surface may have a general affinity for lipid and detergent headgroups. In the intracellular interfacial region the simulation results suggest that two aromatic sidechains (Tyr126 and Tyr189) may form a second lipid headgroup interaction site.

A more detailed analysis of the lipid/protein interactions in simulations OMPT1 and OMPT2 at the proposed LPS site shows little dynamics, with on average one DMPC molecule interacting via the phosphate moiety with each of the Arg138, Arg175 and Lys226 sidechains. It would be interesting to examine whether the diphosphate of Lipid A would form even more stable interactions, possibly with more than one basic sidechain at a time, thus supporting the proposed preferential binding of LPS at this site.

Given the importance of aromatic sidechains in membrane protein interactions with bilayers, we have also analysed the interactions of the two aromatic bands on the surface of OmpT with the phospholipid headgroups. The results for simulations OMPT1 and OMPT2 (Fig. 9) are broadly similar. In both cases, there are rather more aromatic/headgroup interactions at the periplasmic interface than at the extracellular. This analysis also reveals fluctuations in the number of such interactions on a ~2 ns timescale, reinforcing the conclusion above from analysis of numbers of H-bonds.

Overall, these simulations are encouraging in suggesting that 10 ns simulations can reveal key aspects of lipid-protein interactions. Of course, we must remember that the sites in the MD simulations are for interaction with a simple (phosphatidylcholine) bilayer, rather than the more complex lipid environment in the *in vivo* outer membrane. However, the simulation results do enable the formulation of experimentally testable hypotheses as to likely lipid interaction sites on the surface of OmpT.

Discussion

Biological Implications

The results of these simulations appear to support the novel mechanism for OmpT proposed by (Kramer et al., 2001). In particular, they demonstrate that even in the absence of bound peptide, the H212 and D83 sidechains bind a water molecule in an orientation that would favour nucleophilic attack on the scissile peptide bond. Simple peptide docking calculations indicate that a peptide can readily bind in the appropriate orientation at the active site for such a mechanism.

The simulations also reveal the role of water within the β-barrel. Although such water may well play a 'structural' role in stabilizing the transmembrane β-barrel fold, it also seems to be relatively mobile, that is the OmpT barrel forms a water-permeable pore. It is not clear whether or not this has a functional role. It is conceivable that the mobile water within the pore may play a role in 'delivering' water molecules to/from the active site at the external end of the barrel. Alternatively, it may be that the water is playing mainly a structural role and the water permeability of the OmpT barrel is simply tolerated (in an evolutionary sense) given the high permeability of the outer membrane due to the presence of porins. It would be possible to design suitable 'pore-perturbing' mutants that might enable these two alternatives to be tested experimentally.

In terms of interaction of OmpT with its membrane environment, the simulations are quite revelatory. In particular, although the simulations have been performed in a relatively simple DMPC bilayer, they appear to reveal the presence of specific lipid interaction sites on the surface of the OmpT barrel. These sites include the one proposed (Vandeputte-Rutten et al., 2001), on the basis of structural homology with FhuA (Ferguson et al., 2000), to form a site for LPS binding. This result is of interest in terms of revealing the ability of extended MD simulations to provide meaningful information on protein/lipid interactions (Domene et al., 2003b).

Simulation Methodology and Future Directions

From a methodological standpoint these simulations reveal some small differences in behaviour according to whether long range electrostatic interactions are approximated via a simple cutoff or treated more accurately via the PME method. (A more detailed comparison of the effects of this aspect of the methodology on outer membrane protein simulations will be presented elsewhere). However, we note that although more accurate than the cutoff treatment, the PME method is not without possible artefacts (Weber et al., 2000), especially in the context of membrane protein simulations (Bostick and Berkowitz, 2003), which makes some more methodological development in this area desirable.

Our simulation results suggest, in terms of the tilting of the protein relative to the bilayer, that some degree of lipid/protein mismatch may occur for OmpT in DMPC bilayers. More extended simulations are required to obtain a more statistically significant picture of this possible mismatch, and also to explore how the local bilayer geometry may adjust to it. This information could be used to predict experimentally verifiable distances between lipid headgroups and specific protein residues. Given the relaxation time of the protein position in the bilayer this is currently beyond our computational means.

Both this mismatch, and the observation of specific protein/lipid interactions hastens the need for simulations of outer membrane proteins in a more realistic model of the outer membrane than a simple phosphatidylcholine bilayer. Initial modelling and simulation studies of LPS bilayers have been performed (Katowsky et al., 1991; Lins and Straatsma, 2001) and simulations of a more realistic OM model should be feasible in the near future.

The simulations reported here provide valuable clues as to the catalytic mechanism of OmpT. However, in order to characterise this more fully it will be necessary to perform simulations using QM/MM methods (Mulholland et al., 2000; Ridder and Mulholland, 2003). A first approximation to this may be to perform molecular mechanics based simulations that allow for dynamic protonation/deprotonation of water and sidechains (Wu and Voth, 2002).

Acknowledgements.

The authors thank José Faraldo-Gómez for providing the water bridge analysis program and Sundeep Deol for assistance in analysing lipid-protein interactions. MB thanks the EU for a grant (Contract-Nº QLK2-CT-2000-51210). Work in MSPS's laboratory is supported by grants from the Wellcome Trust, the BBSRC and the EPSRC. We thank the Oxford Supercomputing Centre for access to resources.

References

Achouak, W., T. Heulin, and J. M. Pages. 2001. Multiple facets of bacterial porins. *FEMS Microbiol. Lett.* 199:1-7.

Arora, A., F. Abildgaard, J. H. Bushweller, and L. K. Tamm. 2001. Structure of outer membrane protein A transmembrane domain by NMR spectroscopy. *Nature Struct. Biol.* 8:334-338.

Baaden, M., C. Meier, and M. S. P. Sansom. 2003. A molecular dynamics investigation of mono- and dimeric states of the outer membrane enzyme OMPLA. *J. Mol. Biol.* 331:177-189.

Basyn, F., B. Charloteaux, A. Thomas, and R. Brasseur. 2001. Prediction of membrane protein orientation in lipid bilayers: a theoretical approach. *J. Mol. Graphics Modelling.* 20:235-244.

Berendsen, H. J. C., J. P. M. Postma, W. F. van Gunsteren, A. DiNola, and J. R. Haak. 1984. Molecular dynamics with coupling to an external bath. *J. Chem. Phys.* 81:3684-3690.

Berendsen, H. J. C., J. P. M. Postma, W. F. van Gunsteren, and J. Hermans. 1981. Intermolecular Forces. Reidel, Dordrecht.

Berendsen, H. J. C., D. van der Spoel, and R. van Drunen. 1995. GROMACS: A message-passing parallel molecular dynamics implementation. *Comp. Phys. Comm.* 95:43-56.

Bond, P., J. Faraldo-Goméz, and M. S. P. Sansom. 2002. OmpA - A pore or not a pore? Simulation and modelling studies. *Biophys. J.* 83:763-775.

Bond, P., and M. S. P. Sansom. 2003. Membrane protein dynamics vs. environment: simulations of OmpA in a micelle and in a bilayer. *J. Mol. Biol.* 329:1035-1053.

Bond, P. J., and M. S. P. Sansom. 2004. The simulation approach to bacterial outer membrane proteins. *Mol. Memb. Biol.* (in press).

Bostick, D. L., and M. L. Berkowitz. 2003. The implementation of slab geometry for membrane-channel molecular dynamics simulations. *Biophys. J.* 85:97-107.

Buchanan, S. K. 1999. ß-Barrel proteins from bacterial outer membranes: structure, function and refolding. *Curr. Opin. Struc. Biol.* 9:455-461.

Buchanan, S. K., B. S. Smith, L. Venkatramani, D. Xia, L. Essar, M. Palnitkar, R. Chakraborty, D. van der helm, and J. Deisenhofer. 1999. Crystal structure of the outer membrane active transporter FepA from *Escherichia coli*. *Nature Struct. Biol.* 6:56-63.

Caves, L. S. D., J. D. Evanseck, and M. Karplus. 1998. Locally accessible conformations of proteins: Multiple molecular dynamics simulations of crambin. *Protein Sci.* 7:649-666.

Chimento, D. P., A. K. Mohanty, R. J. Kadner, and M. C. Wiener. 2003. Substrate-induced transmembrane signaling in the cobalamin transporter BtuB. *Nat. Struct. Biol.* 10:394-401.

Chinea, G., G. Padron, R. W. W. Hooft, C. Sander, and G. Vriend. 1995. The use of position specific rotamers in model building by homology. *Proteins: Struc. Func. Genet.* 23:415-421.

Cowan, S. W. 1993. Bacterial porins - lessons from 3 high-resolution structures. *Curr. Opin. Struct. Biol.* 3:501-507.

Darden, T., D. York, and L. Pedersen. 1993. Particle mesh Ewald - an N.log(N) method for Ewald sums in large systems. *J. Chem. Phys.* 98:10089-10092.

Dekker, N., R. C. Cox, R. A. Kramer, and M. R. Egmond. 2001. Substrate specificity of the integral membrane protease OmpT determined by spatially addressed peptide libraries. *Biochem.* 40:1694-1701.

Domene, C., P. Bond, and M. S. P. Sansom. 2003a. Membrane protein simulation: ion channels and bacterial outer membrane proteins. *Adv. Prot. Chem.* 66:159-193.

Domene, C., P. J. Bond, S. S. Deol, and M. S. P. Sansom. 2003b. Lipid-protein interactions and the membrane/water interfacial region. *J. Amer. Chem. Soc.* 125:14966-14967.

Faraldo-Gómez, J., G. R. Smith, and M. S. P. Sansom. 2002. Setup and optimisation of membrane protein simulations. *Eur. Biophys. J.* 31:217-227.

Faraldo-Gómez, J., G. R. Smith, and M. S. P. Sansom. 2003. Molecular dynamics simulations of the bacterial outer membrane protein FhuA: a comparative study of the ferrichrome-free and bound states. *Biophys. J.* 85:1-15.

Faraldo-Gómez, J. D., L. R. Forrest, M. Baaden, P. J. Bond, C. Domene, G. Patargias, J. Cuthbertson, and M. S. P. Sansom. 2004. Conformational sampling and dynamics of membrane proteins from 10-nanosecond computer simulations. *Proteins: Struct. Func. Bioinf.* (in press).

Ferguson, A. D., E. Hofmann, J. W. Coulton, K. Diederichs, and W. Welte. 1998. Siderophore-mediated iron transport: crystal structure of FhuA with bound lipopolysaccharide. *Science.* 282:2215-2220.

Ferguson, A. D., W. Welte, E. Hofmann, B. Lindner, O. Holst, J. W. Coulton, and K. Diederichs. 2000. A conserved structural motif for lipopolysaccharide recognition by procaryotic and eucaryotic proteins. *Structure Fold. Des.* 8.

Fernandez, C., C. Hilty, S. Bonjour, K. Adeishvili, K. Pervushin, and K. Wuthrich. 2001. Solution NMR studies of the integral membrane proteins OmpX and OmpA from Escherichia coli. *FEBS Lett.* 504:173-178.

Forst, D., W. Welte, T. Wacker, and K. Diederichs. 1998. Structure of the sucrose-specific porin ScrY from *Salmonella typhimurium* and its complex with sucrose. *Nature Struct. Biol.* 5:37-46.

Fyfe, P. K., K. E. McAuley, A. W. Roszak, N. W. Isaacs, R. J. Codgell, and M. R. Jones. 2001. Probing the interface between membrane proteins and membrane lipids by X-ray crystallography. *Trends Biochem. Sci.* 26:106-112.

Hess, B. 2002. Convergence of sampling in protein simulations. *Phys. Rev. E.* 65:art. no. 031910.

Hess, B., H. Bekker, H. J. C. Berendsen, and J. G. E. M. Fraaije. 1997. LINCS: A linear constraint solver for molecular simulations. *J. Comp. Chem.* 18:1463-1472.

Humphrey, W., A. Dalke, and K. Schulten. 1996. VMD - Visual Molecular Dynamics. *J. Molec. Graph.* 14:33-38.

Hwang, P. M., W. Y. Choy, E. I. Lo, L. Chen, J. D. Forman-Kay, C. R. H. Raetz, G. G. Privé, R. E. Bishop, and L. E. Kay. 2002. Solution structure and dynamics of the outer membrane enzyme PagP by NMR. *Proc. Nat. Acad. Sci. USA.* 99:13560-13565.

Im, W., and B. Roux. 2002. Ions and counterions in a biological channel: A molecular dynamics simulation of OmpF porin from Escherichia coli in an explicit membrane with 1 M KCl aqueous salt solution. *J. Mol. Biol.* 319:1177-1197.

Kabsch, W., and C. Sander. 1983. Dictionary of protein secondary structure:- pattern-recognition of hydrogen-bonded and geometrical features. *Biopolymers.* 22:2577-2637.

Katowsky, M., A. Sabisch, T. Gutberlet, and H. Bradaczek. 1991. Molecular modelling of bacterial deep rough mutant lipopolysaccharide of *Escherichia coli*. *Eur. J. Bioch.* 197:707-716.

Killian, J. A., and G. von Heijne. 2000. How proteins adapt to a membrane-water interface. *Trends Biochem. Sci.* 25:429-434.

Koebnik, R., K. P. Locher, and P. Van Gelder. 2000. Structure and function of bacterial outer membrane proteins: barrels in a nutshell. *Mol. Microbiol.* 37:239-253.

Koronakis, V., A. Sharff, E. Koronakis, B. Luisi, and C. Hughes. 2000. Crystal structure of the bacterial membrane protein TolC central to multidrug efflux and protein export. *Nature.* 405:914-919.

Kramer, R. A., N. Dekker, and M. R. Egmond. 2000. Identification of active site serine and histidine residues in Escherichia coli outer membrane protease OmpT. *FEBS Lett.* 468:220-224.

Kramer, R. A., L. Vandeputte-Rutten, G. J. de Roon, P. Gros, N. Dekker, and M. R. Egmond. 2001. Identification of essential acidic residues of outer membrane protease OmpT supports a novel active site. *FEBS Lett.* 505:426-430.

Krieger, E., G. Koraimann, and G. Vriend. 2002. Increasing the precision of comparative models with YASARA NOVA: a self-parameterizing force field. *Proteins: Struc. Func. Genet.* 47:393-402.

Lavigne, P., J. R. Bagu, R. Boyko, L. Willard, C. F. B. Holmes, and B. D. Sykes. 2000. Structure-based thermodynamic analysis of the dissociation of protein phosphatase-1 catalytic subunit and microcystin-LR docked complexes. *Prot. Sci. 9.* 9:252-264.

Lee, A. G. 2003. Lipid-protein interactions in biological membranes: a structural perspective. *Biochim. Biophys. Acta.* 1612:1-40.

Lindahl, E., and O. Edholm. 2000. Mesoscopic undulations and thickness fluctuations in lipid bilayers from molecular dynamics simulations. *Biophys. J.* 79:426-433.

Lins, R. D., and T. P. Straatsma. 2001. Computer simulation of the rough lipopolysaccharide membrane of *Pseudomonas aeruginosa*. *Biophys. J.* 81:1037-1046.

Locher, K. P., B. Rees, R. Koebnik, A. Mitschler, L. Moulinier, J. Rosenbusch, and D. Moras. 1998. Transmembrane signalling across the ligand-gated FhuA receptor; crystal structures of free and ferrichrome-bound states reveal allosteric changes. *Cell.* 95:771-778.

Merritt, E. A., and D. J. Bacon. 1997. Raster3D: Photorealistic molecular graphics. *Methods Enzymol.* 277:505-524.

Morris, G. M., D. S. Goodsell, R. S. Halliday, R. Huey, W. E. Hart, R. K. Belew, and A. J. Olson. 1998. Automated docking using a Lamarckian genetic algorithm and an empirical binding free energy function. *J. Comp. Chem.* 19:1639-1662.

Mulholland, A. J., P. D. Lyne, and M. Karplus. 2000. Ab initio QM/MM study of the citrate synthase mechanism. A low-barrier hydrogen bond is not involved. *J. Am. Chem. Soc.* 122:534-535.

Nielsen, J. E., and G. Vriend. 2001. Optimizing the hydrogen-bond network in Poisson-Boltzmann equation- based pK(a) calculations. *Proteins: Struc. Func. Genet.* 43:403-412.

Ridder, L., and A. J. Mulholland. 2003. Modeling biotransformation reactions by combined quantum mechanical/molecular mechanical approaches: from structure to activity. *Curr. Topics Med. Chem.* 3:1241-1256.

Schirmer, T. 1998. General and specific porins from bacterial outer membranes. *J. Struct. Biol.* 121:101-109.

Schirmer, T., T. A. Keller, Y. F. Wang, and J. P. Rosenbusch. 1995. Structural basis for sugar translocation through maltoporin channels at 3.1A resolution. *Science.* 267:512- 514.

Snijder, H. J., I. Ubarretxena-Belandia, M. Blaauw, K. H. Kalk, H. M. Verheij, M. R. Egmond, N. Dekker, and B. W. Dijkstra. 1999. Structural evidence for dimerization-regulated activation of an integral membrane phospholipase. *Nature.* 401:717-721.

Sugimura, K., and T. Nishihara. 1988. Purification, characterization, and primary structure of Escherichia coli protease VII with specificity for paired basic residues: identity of protease VII and OmpT. *J. Bacteriol.* 170:5625-5632.

Tieleman, D. P., and H. J. C. Berendsen. 1998. A molecular dynamics study of the pores formed by *Escherichia coli* OmpF porin in a fully hydrated palmitoyloleoylphosphatidylcholine bilayer. *Biophys. J.* 74:2786-2801.

van Gunsteren, W. F., and H. J. C. Berendsen. 1987. Gromos-87 manual. Biomos BV, Groningen.

Vandeputte-Rutten, L., R. A. Kramer, J. Kroon, N. Dekker, M. R. Egmond, and P. Gros. 2001. Crystal structure of the outer membrane protease OmpT from *Escherichia coli* suggests a novel catalytic site. *EMBO J.* 20:5033-5039.

Wallace, A. C., R. A. Laskowski, and J. M. Thornton. 1995. LIGPLOT: a program to generate schematic diagrams of protein-ligand interactions. *Prot. Engng.* 8:127-134.

Weber, W., P. H. Hunenberger, and J. A. McCammon. 2000. Molecular dynamics simulations of a polyalanine octapeptide under Ewald boundary conditions: Influence of artificial periodicity on peptide conformation. *J. Phys. Chem. B.* 104:3668-3675.

Wu, Y., and G. Voth. 2002. Computer simulation studies of proton transport in a synthetic ion channel. *Biophys. J.* 82:1016.

Tables

Table 1: Summary of Simulations

Name	PME or Cutoff	Duration (ns)	Cα RMSD* (Å)	
			β-strands	Not β-strands
OMPT1	PME	10	1.00 ± 0.07	2.61 ± 0.24
OMPT2	Cutoff	10	1.20 ± 0.08	3.58 ± 0.28
OMPT3a	Cutoff	2.5	0.72 ± 0.05	1.85 ± 0.32
OMPT3b	Cutoff	2.5	0.77 ± 0.06	2.12 ± 0.31
OMPT3c	Cutoff	2.5	0.94 ± 0.15	2.05 ± 0.43

*The Cα RMSD is calculated, relative to the starting structure, for the final 2 ns of each simulation. Each simulation system consisted of 63205 atoms, corresponding to monomeric OmpT, 19 water molecules taken from the X-ray structure, 33 Na^+ ions, 30 Cl^- ions, 249 lipid (DMPC) molecules and 16191 waters in total.

Table 2: H-bond Interactions at the Active Site

Interaction	OMPT1	OMPT2	OMPT3a	OMPT3b	OMPT3c
D210-H212	100	100	100	100	100
D210-E27	-	-	1.6	40.5	-
D83-S99	7.0	31.9	2.4	13.5	31.7
D83-H101	-	31.5	2.4	1.6	0.8
D83-w-H212	15.8	52.1	78.6	67.5	49.2
D83-w-D85	72.9	58.1	93.7	81.7	96.0
D85-S40	81.4	55.7	77.0	93.7	98.4

The values indicate percentages of total simulation time for which a given H-bond was present. An interaction is recorded only if it was present for >30% in at least one simulation.

Table 3: Dominant Lipid/Protein Interactions

Interaction	OMPT1	OMPT2	OMPT3a	OMPT3b	OMPT3c
Proposed site					
ARG138	97.0	85.4	67.5	95.2	88.9
ARG175	26.1	33.3	93.7	99.2	13.5
LYS226	0.0	91.0	90.5	100.0	85.7
TYR134	39.9	0.0	99.2	0.0	0.0
E136-w	62.6	92.2	98.2	97.6	95.6
Vicinity					
LYS177	96.0	46.3	100.0	92.1	33.3
2nd site					
ARG77	100.0	95.4	69.0	83.3	93.7
ARG255	60.1	76.8	84.9	0.0	7.1
ASN47	94.0	100.0	48.4	95.2	10.3
Lower belt					
TYR189	77.8	94.2	100.0	8.7	33.3
TYR126	9.8	98.2	52.4	5.6	100.0
THR2	55.3	36.1	0.0	0.0	0.0

Protein-lipid interactions (given as percentage of total simulation time for which an H-bonding interaction is formed between the phosphate of DMPC and a protein sidechain) are listed for: (i) 'proposed site' = residues identified by analogy with the Fhua LPS binding site; (ii) 'vicinity' = interactions with Lys177 which sits near to the proposed site; (iii) '2nd site' = a putative second LPS-binding site; and (iv) 'lower belt' = interactions with the lower (periplasmic) half of the protein.

Figures

Figure 1:

A OmpT fold showing: (i) the four active site residues (i.e. Asp83, Asp85 on the left, and Asp210, His212 on the right) in red; (ii) the basic lipid binding sites formed by Arg and Lys residues in orange; and (iii) the upper and lower amphipathic aromatic belts formed by Trp and Tyr residues in green. The position of the lipid bilayer is delineated by horizontal lines, with the extracellular space located at the top and the periplasm at the bottom. **B** A schematic cross-section of OmpT indicating the approximate position of a potential tetrapeptide substrate (in black). **C** Snapshots from the OMPT2 simulation at t = 0 and 10 ns. The protein is blue (cartoon representation), the lipid bilayer polar headgroups are shown as red and orange spheres, the hydrophobic tails as green lines, water molecules as blue dots, and Na^+ and Cl^- ions as purple and cyan spheres respectively. Three regions are indicated: w = water, i = interface; h = hydrophobic core.

Figure 2:

Root Mean Square Deviation (RMSD) of Cα atoms from the starting structure *vs.* time for the OmpT1 (**A**) and OmpT2 (**B**) simulations. The RMSD for all residues (black lines, labelled 'all'), for the loop and turn residues (light grey lines, labelled 'loops') and for secondary structure (i.e. β-sheet) elements (dark grey lines, labelled 'barrel') are shown.

Figure 3:

A Root Mean Square Fluctuations (RMSF) of Cα atoms *vs.* residue number for the OmpT1 simulation (black line) compared to fluctuations derived from the crystallographic B-factors

(blue line). The background of the graph is coloured according to secondary structure (pink = β-strand; yellow = loop) and the β-strands are labelled.

B Superimposed protein structures from the OMPT1 and OMPT2 trajectories (showing frames saved every 0.4 ns) highlighting regions of high flexibility. Structures are coloured according to the frame number from blue (start, 0 ns) via green to red (end, 10 ns).

C Dominant secondary structure analysis for simulations OMPT1, OMPT2 and OMPT3 showing residues that maintain their secondary structure as determined via DSSP (Kabsch and Sander, 1983) for more than 90% of the total simulation time. Red = β-strand, green = bend, yellow = turn, light grey = coil. The β-strands and extracellular loops are labelled.

Figure 4:

A Selected snapshot of important active site residues (D83, D85, H212, D210, E27, D208, S99) in a representative conformation, in particular showing the interactions E27-D208, H212-water-D83 and D83-water-D85.

B Superposed on a line representation of the conformation shown in **A** are snapshots of: an E27-water-D210 interaction (in purple), a conformation where H212 is more distant from D83 which in turn is interacting with S99 (in orange), and a conformation where D85 is far from D83 (in brown).

C Interaction existence plot where a given H-bonding interaction is plotted *vs.* time. The first three lines correspond to interactions of D83 with H212 via a water bridge, with S99 and with D85 via water bridges. The colours are black for a single interaction, red for two bridging waters, blue for three and green for four water bridges. The last two lines show the possible interactions of E27, with either D208 or via water bridges with D210.

Figure 5:

Results of docking calculations, showing a selected OmpT-ARRA complex in which interacting protein residues are in light blue, the peptide is in green, and the scissile peptide bond is highlighted in yellow. D83 is protonated and a water molecule between D83 and H212 is shown. The putative catalytic mechanism is indicated via arrows. The I170 residue is not shown for clarity, but its approximate sidechain position is indicated by an asterisk.

Figure 6:

A Diagram of the cumulative water density inside the OmpT barrel, taken from the OMPT1 trajectory. Two orthogonal views are shown.

B Trajectory of a single water molecule leaving the central pocket towards the periplasmic space.

C Selected water trajectories from the OMPT1 simulation projected onto the *z* axis. The approximate limits of the transmembrane region are shown as black horizontal lines. The blue trajectory corresponds to the water molecule shown in **B**.

Figure 7:

The number of OmpT/lipid H-bonds *vs*. time for simulations OMPT1 (black line) and OMPT2 (grey line).

Figure 8:

A Comparison of the covalent structures of DMPC *vs.* lipid A (the latter after (Ferguson et al., 2000)).

B Snapshots showing the interactions between basic residues and DMPC at the putative lipid A binding site for the three residues Lys226, Arg175 and Arg138.

Figure 9:

Contour plot of the number of interactions (≤ 3.5 Å) of the amphipathic aromatic (i.e. Tyr, Trp) residues of OmpT with lipid polar headgroups as a function of position in the bilayer *vs.* time for simulations **A** OMPT1 and **B** OMPT2.

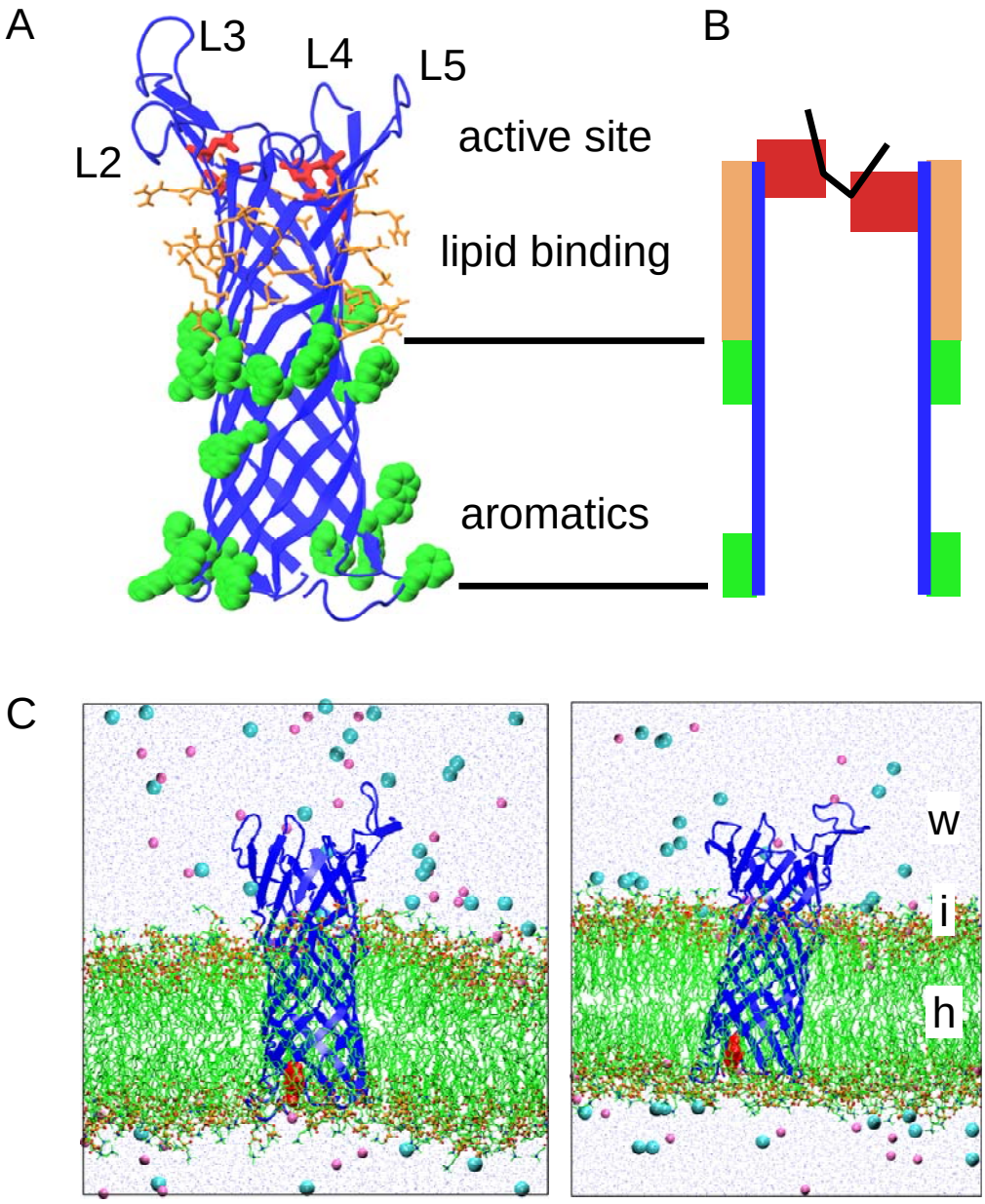
A
L3
L4
L5
L2
active site
lipid binding
aromatics
B
C
w
i
h

Baaden & Sansom, Fig. 2

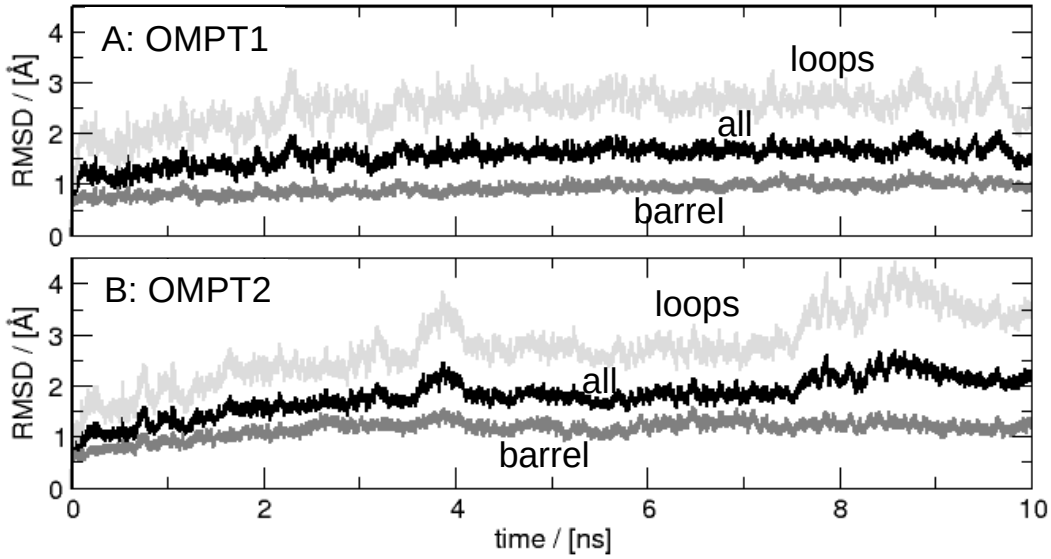

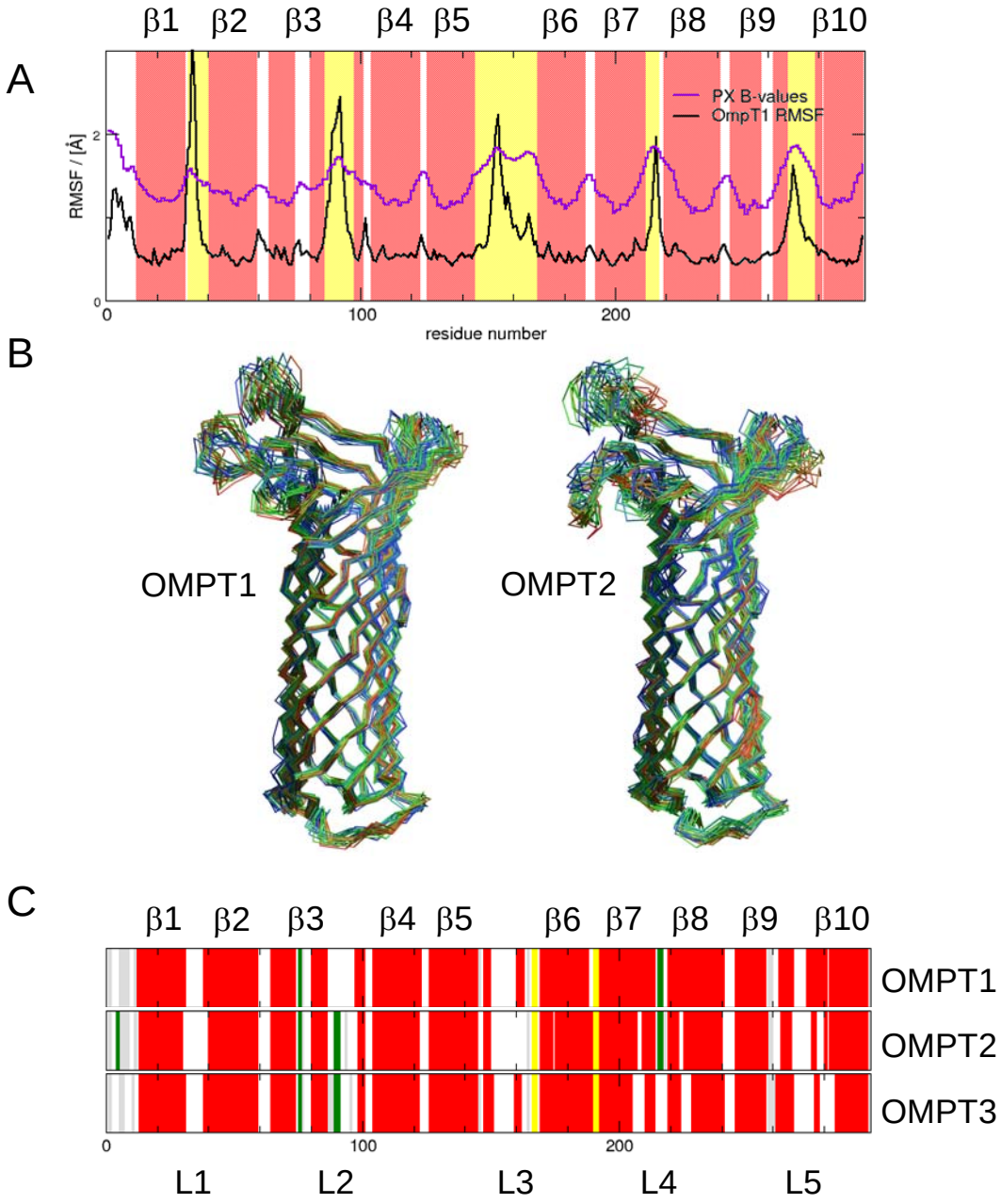
A
β1 β2 β3 β4 β5 β6 β7 β8 β9 β10
PX B-values
OmpT1 RMSF
RMSF / [Å]
residue number
B
OMPT1
OMPT2
C
β1 β2 β3 β4 β5 β6 β7 β8 β9 β10
OMPT1
OMPT2
OMPT3
L1 L2 L3 L4 L5

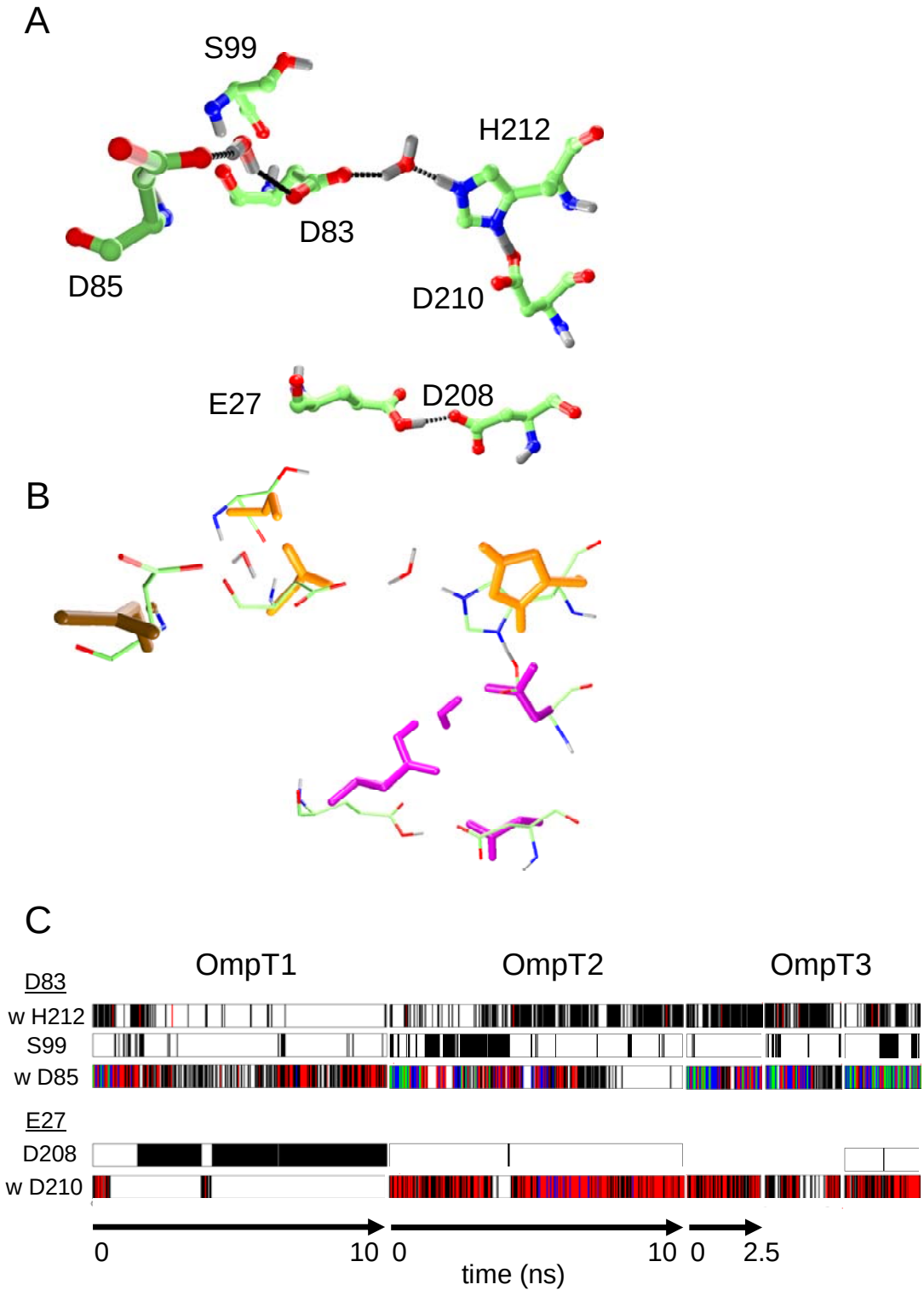
A
S99
H212
D83
D85
D210
E27
D208
B
C
OmpT1
OmpT2
OmpT3
D83
w H212
S99
w D85
E27
D208
w D210
0
10
0
10
0
2.5
time (ns)

Baaden & Sansom, Fig. 5

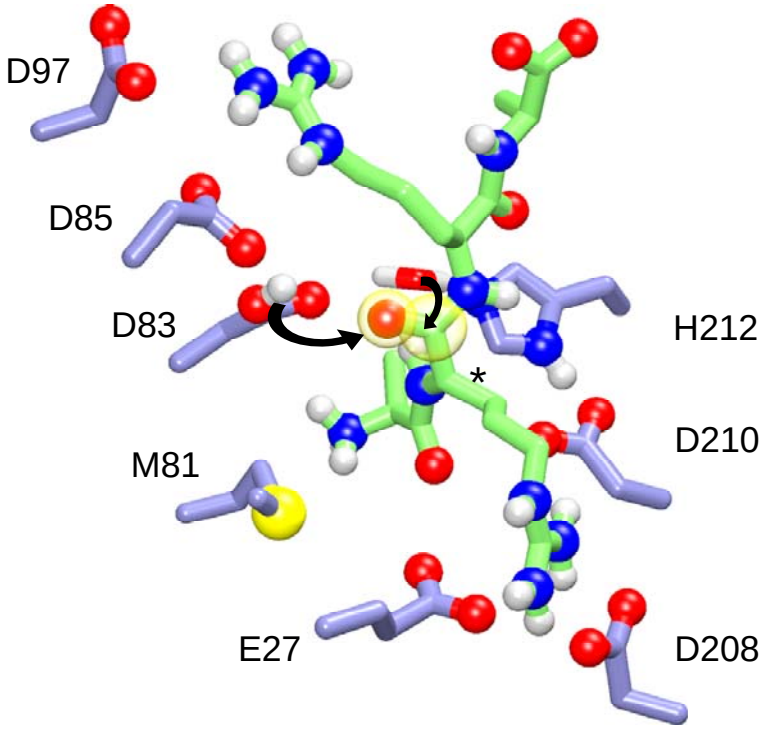

Baaden & Sansom, Fig. 6

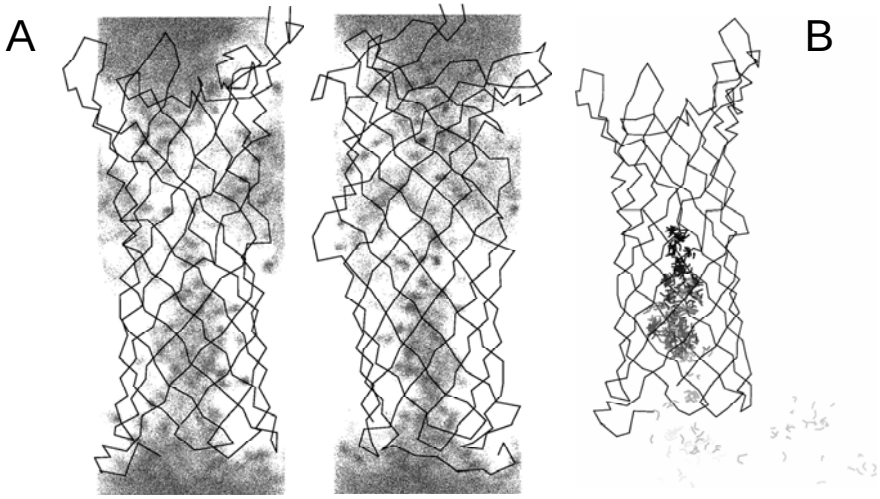

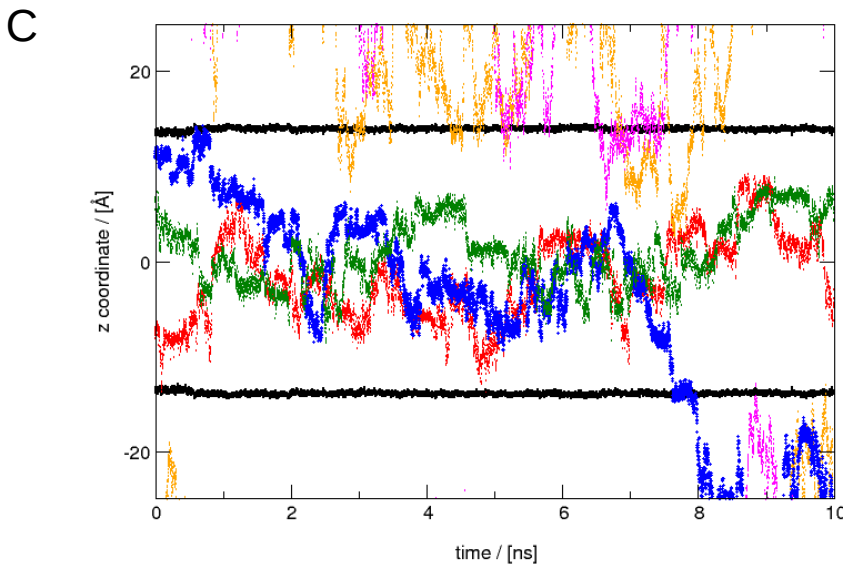

Baaden & Sansom, Fig. 7

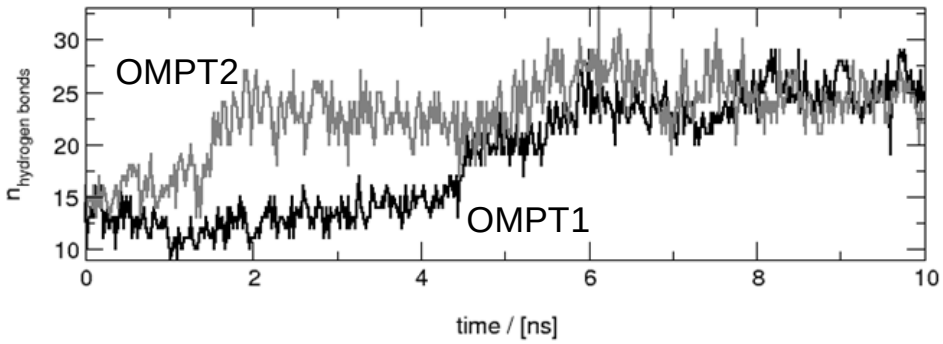

Baaden & Sansom, Fig. 8

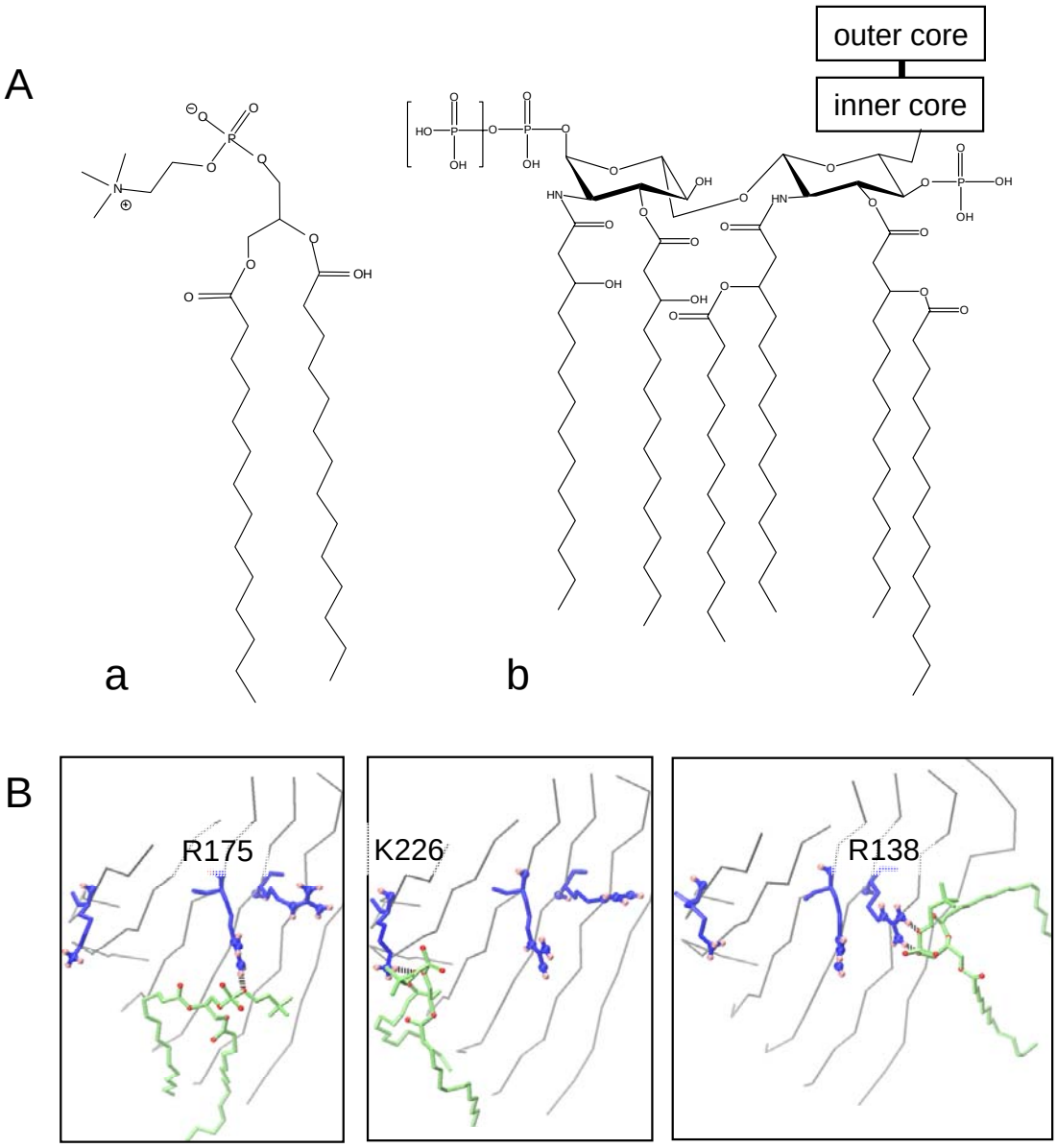

Baaden & Sansom, Fig. 9